J. Microbiol. Biotechnol. (2007), **17**(9), 1504–1512

JOURNAL OF MICROBIOLOGY AND BIOTECHNOLOGY

Molecular Characterization of FprB (Ferredoxin-NADP$^+$ Reductase) in *Pseudomonas putida* KT2440

LEE, YUNHO[1], JINKI YEOM[1], YOON-SUK KANG[1], JUHYUN KIM[1], JUNG-SUK SUNG[2], CHE OK JEON[3], AND WOOJUN PARK[1,3]*

[1]*Division of Environmental Science and Ecological Engineering, Korea University, Seoul 136-701, Korea*
[2]*Department of Life Science, Dongguk University, Seoul 100-715, Korea*
[3]*Division of Applied Life Science, EB-NCRC, PMBBRC, Gyeongsang National University, Jinju 660-701, Korea*

Received: April 7, 2007 Accepted: June 1, 2007

Abstract The *fpr* gene, which encodes a ferredoxin-NADP$^+$ reductase, is known to participate in the reversible redox reactions between NADP$^+$/NADPH and electron carriers, such as ferredoxin or flavodoxin. The role of Fpr and its regulatory protein, FinR, in *Pseudomonas putida* KT2440 on the oxidative and osmotic stress responses has already been characterized [Lee *at al.* (2006). *Biochem. Biophys. Res. Commun.* 339, 1246–1254]. In the genome of *P. putida* KT2440, another Fpr homolog (FprB) has a 35.3% amino acid identity with Fpr. The *fprB* gene was cloned and expressed in *Escherichia coli*. The diaphorase activity assay was conducted using purified FprB to identify the function of FprB. In contrast to the *fpr* gene, the induction of *fprB* was not affected by oxidative stress agents, such as paraquat, menadione, H_2O_2, and *t*-butyl hydroperoxide. However, a higher level of *fprB* induction was observed under osmotic stress. Targeted disruption of *fprB* by homologous recombination resulted in a growth defect under high osmotic conditions. Recovery of oxidatively damaged aconitase activity was faster for the *fprB* mutant than for the *fpr* mutant, yet still slower than that for the wild type. Therefore, these data suggest that the catalytic function of FprB may have evolved to augment the function of Fpr in *P. putida* KT2440.

Keywords: Oxidative stress, ferredoxin, osmotic stress, aconitase

Ferredoxin-NADP$^+$ reductases (Fpr) are known to mediate reversible electron exchange between NADP(H) and one-electron carriers, such as the iron-sulfur protein ferredoxin [3]. Ferredoxin is present in all organisms, including bacteria and archaea [30]. In oxygenic photosynthesis, photosystem I-reduced ferredoxin (Fd) passes electrons on to NADP$^+$ via Fpr. This reaction then provides the NADPH needed for CO_2 assimilation and other biosynthetic routes [4]. Reduced ferredoxin, owing to the reverse enzymatic activity of Fpr, can donate an electron to several Fd-dependent enzymes, such as nitrite reductase, sulfite reductase, glutamate synthase, and Fd-thioredoxin reductase, allowing ferredoxin to function in a variety of systems, including oxidative stress [30]. Furthermore, ferredoxin is known to be involved in the assembly of iron-sulfur clusters [8].

Fpr also catalyzes irreversible electron transfer, the so-called diaphorase reaction, which drives the oxidation of NADPH in a wide variety of adventitious electron acceptors, such as viologens, quinines, complexed transition metals, and tetrazolium salts [21]. However, the physiological role of Fpr during normal growth remains to be fully elucidated. In *E. coli* and *Salmonella*, the *fpr* gene belongs to the SoxRS regulon [12], and it has been proposed that Fpr modulates the NADP(H) levels during the *soxRS* response of *E. coli*, as Fpr depletion in *fpr* mutant cells may be linked to an abnormal increase in the NADPH levels, thereby increasing the production of highly toxic hydroxyl radicals. Moreover, the involvement of Fpr in the reactivation of oxidized hydrolyase, such as aconitase, 6-phosphogluconate dehydrogenase, has also been recently shown [10].

Previously, the *fpr* gene was reported not to be regulated by the SoxRS system in *P. putida* KT2440 [26], whereas the expression of *fpr* was induced by FinR, a LysR-type transcriptional factor near the *fpr* gene in the chromosome [21]. *P. putida* KT2440 deficient in *fpr* displays an abnormal sensitivity to oxidative and osmotic stress [21]. Accordingly, in the present study, FprB, the second *fpr* homolog, was expressed at high levels in *E. coli*, and then purified to verify its function. The expression and function of *fprB* were also examined under various conditions, including the requirement of FinR or LuxR, a putative transcriptional regulator, near *fprB* for its induction.

*Corresponding author
Phone: 82-2-3290-3067; Fax: 82-2-953-0737;
E-mail: wpark@korea.ac.kr

MATERIALS AND METHODS

Bacterial Strains, Plasmids, and Growth Conditions

The bacterial strains, plasmids, and primers used in this study are listed in Table 1. Antibiotics (kanamycin, 100 μg/ml; tetracycline, 20 μg/ml; rifampicin, 200 μg/ml; ampicillin, 50 μg/ml) were added when necessary.

DNA Manipulation and Molecular Cloning

A 356-bp fragment of the internal region of the *fprB* gene that had been amplified using FprB-KO1/-KO2 primers was cloned into the EcoRI cloning site of a pVIK112 [17] vector, generating pVIK-*fprB* (Table 1). The construction of an *fprB* mutant of *P. putida* KT2440 using homologous recombination was then performed as described previously [21]. The suicide vector pCVD442 [27] was used to construct a *luxR* mutant, and the LuxR-KO1/-KO2 primer pair used to target the internal region of the *luxR* gene. The resulting amplified 688-bp fragment was then subcloned into the EcoRI cloning site of pCR2.1, creating pCR2.1-*luxR*, and the *luxR* gene in pCR2.1-*luxR* inactivated *in vitro* by the insertion of the kanamycin cassette from pUC4K

Table 1. Bacterial strains, plasmids, and primers used in this study.

Bacterial strain/plasmid	Description	Reference
Strains		
E. coli S17-1λ*pir*	Tra+ R6K strain, used for biparental conjugation	Lab stock
E. coli Top10	*mcrA, Δ(mrr-hsdRMS-mcrBC), Φ80lacZΔM15*	Promega
E. coli BL21(DE3)	F- *ompT hsdS*B (rB^-mB^-) *gal dcm* (DE3)	Invitrogen
P. putida KT2440-R	Rifampicin-resistant strain of *P. putida* KT2440	[21]
P. putida KT2440-*fprB*	*fprB* mutant, insertion of pVIK-*fprB* into *P. putida* KT2440	This study
P. putida KT2440-*fpr*	*fpr* mutant, insertion of pVIK-*fpr* into *P. putida* KT2440	[21]
P. putida KT2440-*luxR*	*luxR* mutant, insertion of *luxR*::Km into *P. putida* KT2440 by double crossover	This study
P. putida KT2440- P_{fprB}-*lacZ*	P_{fprB}-lacZ fusion in chromosome of *P. putida* KT2440	This study
P. putida KT2440 (pRK415-P_{fprB})	P_{fprB} -gfp fusion in *P. putida* KT2440	This study
Plasmids		
pVIK112	R6K*oriV*, suicide vector, *lacZ* fusion	[17]
pCR2.1 TOPO	TA cloning vector	Invitrogen
pUC4K	Kanamycin resistance gene	[24]
pCVD442	R6K *ori, mobRP4, bla, sacB*	[27]
pRK415gfp	Broad-host-range vector, Tet^R, Mob^+	[31]
pRK415*fprB*::*gfp*	Internal *fprB* fragment region in pRK415	This study
pVIK-*fprB*	Internal *fprB* fragment region in pVIK112	This study
pCR2.1-*luxR*	Internal *luxR* fragment region in pCR2.1	This study
pCR2.1-*luxR*::*Km*	1.2-kb fragment containing Km cassette in *luxR* fragment region in pCR2.1-*luxR*	This study
pCVD442-*luxR*::*Km*	1.2-kb fragment containing Km cassette in *luxR* fragment region in pCVD442	This study
pVIK112-P_{fprB}	Promoter region of *fprB* in pVIK112	This study
pRK415-P_{fprB}	Promoter region of *fprB* in pRK415gfp	This study
pET-28a(+)	Protein overexpression with His taq	Novagen
pET-*fprB*	*fprB* fragment region in pET-28 a(+)	This study
Primers	Sequence 5'-3'	
FprB-KO1	CGC GAA TTC CAG GCG TTT GGT TTT CTC AC	
FprB-KO2	CGC GAA TTC AGC CCT GCC GCC TTC TCC	
LuxR-KO1	CGC GAA TTC GGA CCT GGA CAT GGA TTA CCT T	
LuxR-KO2	CGC GAA TTC GCT TTG CCG GGC GAT TCT A	
PfprB-pro1	CGC GAA TTC GCG GTC ATA TCG GGC TCC AG	
PfprB-pro2	CGC GAA TTC CCC AAG GTA ATC CAT GTC CAG GTC	
PluxR-pro1K	CGC GGT ACC GCG GTC ATA TCG GGC TCC AG	
MCS-R	ACC ATG GTC ATA GCT GTT TCC TG	
Pgfp-down	CGC AAG CTT ATT TGT ATA GTT CAT CCA TGC	
FprB-OE1	CGC CAT ATG ACC GCT AGC GCC GAA AAG TTC A	
FprB-OE2	CGC GTC GAC CAC AAC GGC CGC AAT GGT C	

*Underlined restriction site for cloning.

[24]. Thereafter, the pCR2.1-*luxR* plasmid was digested with ClaI, and then filled with a Klenow fragment to create blunt ends. A BamHI fragment, containing the Km cassette from pUC4K [24], was also filled with a Klenow fragment to create blunt ends, and then ligated with the blunt-ended pCR2.1-*luxR* plasmid to form pCR2.1-*luxR*::Km. The *luxR*::Km cartridge was liberated using EcoRI, and then ligated into the EcoRI cloning site of pCVD442 to create pCVD442-*luxR*::Km. Thus, the construction of a *luxR* mutant of *P. putida* KT2440 using homologous recombination was performed as described above. *P. putida* KT2440-P_{fprB}-*lacZ* and *P. putida* KT2440 (pRK415-Pf_{prB}) were used to monitor the expression of the *fprB* gene under osmotic conditions. The promoter region of the *fprB* gene was amplified using the PfprB-pro1/-pro2 primer pair (yielding a 355-bp fragment), and then cloned into the EcoRI cloning site of a pVIK112 vector, generating pVIK112-P*fprB*. Thus, *P. putida* KT2440-P_{fprB}-*lacZ* was created as described above. A broad-host-range promoter probe vector, pRK415gfp [31], was used to construct a reporter plasmid, pRK415-Pf_{prB}, which was then introduced into *P. putida* KT2440-R to create *P. putida* KT2440 (pRK415-Pf_{prB}).

Protein Purification Conditions

The open reading frame of the *fprB* gene was amplified by a PCR using the FprB-OE1/-OE2 primer pair (yielding a 798-bp fragment). The amplified fragment containing the *fprB* gene was then cloned into the NdeI/SalI sites of pET-28a(+) , yielding pET-*fprB*. Thereafter, the pET-*fprB* was transformed into *E. coli* BL21 (DE3) cells by electroporation, and the *E. coli* BL21(DE3) cells harboring the pET-*fprB* were grown under moderate shaking at various temperatures in a 2× YT medium supplemented with kanamycin (100 μg/ml). For enzyme purification, the *E. coli* cells were grown to the mid-log phase (OD_{600}~0.7) at 30°C with aeration. The cell cultures were grown at 25°C for 5–7 h after induction with 0.2 mM isopropyl thio-D-galactoside (IPTG), and then harvested. All the purification steps were performed at 4°C using a fast protein liquid chromatography (FPLC) system (AKTA Purifier 10, UNICORN 4.0, Amersham Bioscience). The *E. coli* cell pellets were resuspended in 50 mM Tris/Cl (pH 8.0) and disrupted by sonication. After removing the cell debris by centrifugation at 12,000 ×*g* for 10 min, the soluble fraction was loaded onto a column. The pellets were resuspended in a Tris/Cl (pH 8.0) buffer and applied to a DEAE column (1 ml, DEAE-Sepharose, Amersharm Bioscience) equilibrated with the same buffer, and the proteins eluted with a 20-ml linear gradient of 0–1 M NaCl in a 50 mM Tris/Cl buffer (pH 8.0). The fractions (0.5 ml each) were collected and concentrated by ultrafiltration using 2 ml of YM-10 Amicon. The concentrate was then divided into two 0.5-ml fractions, and each fraction applied to a gel-permeation column (Sephacryl S-300 HR 16/60, Pharmacia) equilibrated with a 50 mM Tris/Cl buffer (pH 8.0) containing 150 mM NaCl. The proteins were eluted from the column using the same buffer at a flow rate of 30 ml/h. SDS-PAGE was also carried out on 10% polyacrylamide gels to check the level of expression. The molecular mass of the native FprB protein was measured using size exclusion chromatography (Sephacryl S-200 HR 16/60, Pharmacia), which was previously calibrated with alcohol dehydrogenase (150 kDa), bovine serum albumin (67 kDa), and lysozyme (14 kDa) as known monomeric proteins, at a flow rate of 30 ml/h [16, 32].

Diaphorase Activity Assay

The diaphorase activity was measured in 0.1 M Tris/Cl (pH 8.0) at room temperature with 2,6-dichlorophenol-indophenol (DPIP) as the electron acceptor and NADPH as the electron donor. The NADPH concentration was kept constant by regeneration using 2.4 mM glucose-6-phosphate and 1.45 U glucose-6-phosphate dehydrogenase [9]. The cells transformed with pET-28a(+) (Control) and pET-*fprB* (Over-FprB) were harvested by centrifugation at 14,000 ×*g* for 20 min, and then the pellets were resuspended in 20 mM Tris/Cl (pH 8.0) and disrupted by sonication. After removing any cell debris by centrifugation at 12,000 ×*g* for 10 min, the proteins (0.4 μg) in the soluble fraction were used in the DPIP activity assay [28]. The reduction of DPIP, based on the decrease of absorbance at 600 nm (ε_{600}=21.8 mM/cm), was continuously monitored on a Mecasys Optizen 2120 UV/VIS spectrophotometer.

Northern Blot Analysis

Total RNA was isolated from 2 to 3 ml of exponentially growing cells using an RNeasy Mini kit (Qiagen) according to the manufacturer's instructions. A Northern blot analysis was then performed as described previously [18, 21].

β-Galactosidase and GFP Fluorescence Measurement

Bacterial cells with the P_{fprB}-*lacZ* or P_{fprB}-*gfp* fusion were collected from a 3-day culture grown on either NaCl-free LB or NaCl-containing LB plates (0.17 M or 0.85 M NaCl). The β-galactosidase activities of the bacterial cultures were then determined using the method described by Miller [23]. The GFP fluorescence intensity was quantified using a microtiter plate reader (VICTOR^3, Biorad), as described previously [20].

Aconitase Activity Assay

The wild type, *fpr*, and *fprB* mutant cells were precultured at 30°C in an LB medium. One-hundred μM of paraquat was then added to early exponentially grown cells (OD_{600}~0.4–0.5), followed by incubation for 30 min, and then the cells were harvested and washed with PBS. Next, the collected cells were resuspended in the same medium and incubated under the same conditions, but without agitation. The protein concentration was quantified using the Bradford method,

and the aconitase activity measured spectrophotometrically at 240 nm at room temperature by monitoring the production of *cis*-aconitate (ε240=3.6 mM/cm). The assays (1 ml volume) were conducted in 90 mM Tris/Cl (pH 8.0), and the reactions initiated by the addition of 20 mM sodium isocitrate. One unit of aconitase activity was defined as the amount of *cis*-aconitate converted/min/mg of protein.

RESULTS AND DISCUSSION

Identification of *fprB* Gene in *P. putida* KT2440 Genome

In previous studies by the current authors, the *fpr* gene was characterized as being highly induced by oxidative as well as osmotic stress, whereas its expression was dependent on the presence of FinR, a LysR-type transcriptional factor near the *fpr* gene in the chromosome [21]. A database search of the *P. putida* KT2440 genome identified a second Fpr homolog, a putative ferredoxin-NADP$^+$ reductase (FprB), with a 35.3% amino acid identity with the Fpr of *P. putida* KT2440. An analysis of the Fpr homologs in the database revealed that *P. aeruginosa* PAO1 and *P. syringae* pv. tomato DC3000 also had two *fpr* genes, whereas *E. coli* and *Salmonella* only had one *fpr* gene that is known to be a member of the SoxR regulon [11]. The chromosomal loci with genes encoding the *fprB* homologs in various microorganisms are shown in Fig. 1A, where the organization of the *fprB* region in *P. aeruginosa* differs from that in the two other *Pseudomonas* species, as a putative LuxR homolog is absent in *P. aeruginosa*. A gene annotated as a PA4616 (probable c4-dicarboxylate-binding protein) near a putative oxidoreductase in the *P. aeruginosa* chromosome has a very low amino acid identity (12.2%) with the LuxR of *P. putida* KT2440 [*P. aeruginosa* McsL, 91.9%; putative oxidoreductase (FprB), 82.9%; PA4617 (methyl transferase), 77.8% amino acid identities with those of *P. putida* KT2440, respectively]. Interestingly, the upstream region of *fprB* in *P. syringae* has a transposase-like gene, suggesting that this region may have previously been transferred in the form of a composite transposon in *P. syringae*. Moreover, the *fprB* gene from *P. putida* KT2440 has an 82.9% amino acid identity with the *fprB* gene from *P. syringae*.

When the Fpr and FprB proteins were analyzed using *Azotobacter* subclass I ferredoxin reductase and *E. coli* subclass II ferredoxin reductase, FprB was found to contain aromatic residues within the carboxyl terminal

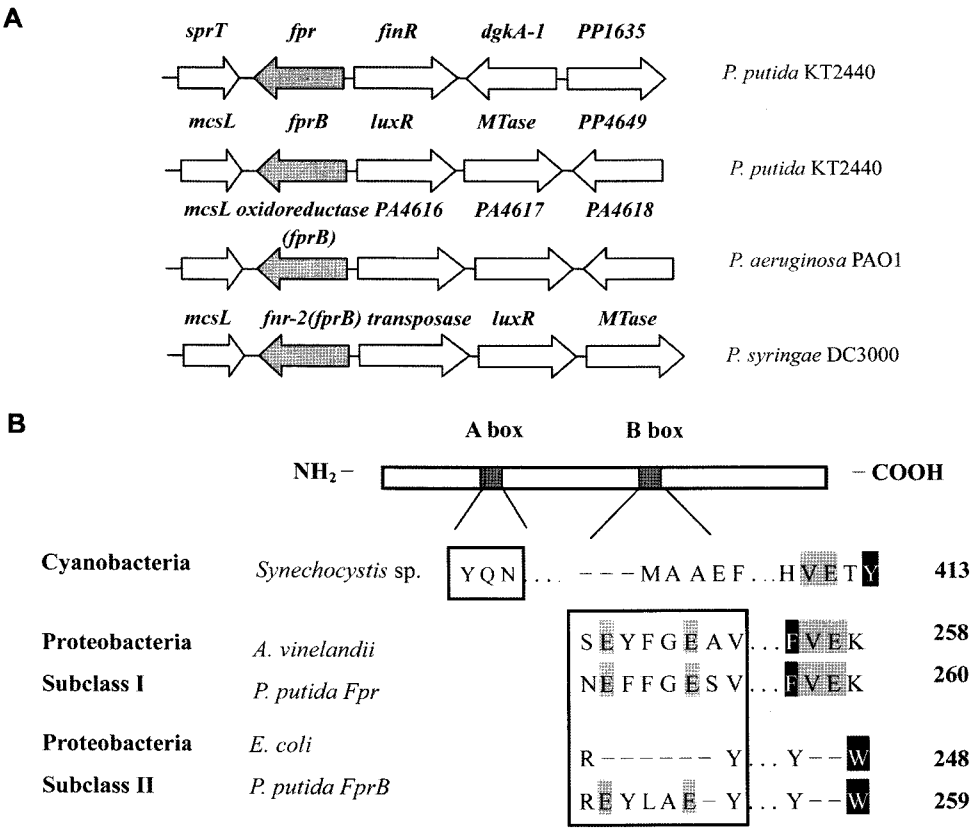

Fig. 1. A. Genetic organization of *fprB* homologs among *Pseudomonas* strains. PA4616: probable c4-dicarboxylate-binding protein. **B.** Conserved regions of various bacterial ferredoxin-NADP$^+$ reductases.
The numbers indicate the number of amino acids in each bacterial ferredoxin reductase; a gray color indicates conserved amino acids that appear more than three times in five ferredoxin reductases, including plastidic ferredoxin reductase; and a black box indicates functionally important amino acid residues.

domains and tryptophan residues at the C-terminal end, whereas Fpr possessed aliphatic C-terminal domains and phenylalanine at the C-terminal end (Fig. 1B, black box). However, Fpr and FprB both lacked an "A box", a structural characteristic of a plastidic (chloroplasts, cyanobacteria) ferredoxin reductase [5], implying that the FAD prosthetic group exists in a folded conformation [5]. A tyrosine residue in an "A box" is one of the criteria of a plastidic ferredoxin reductase, which was also missing in the bacterial enzymes (Fig. 1B, black box). The presence of a gap in a "B box", a structural feature of a subclass II bacterial reductase [5], was not obvious in the FprB amino acid sequence. However, a sequence analysis of the FprB C-terminal domain suggested that FprB may be a subclass II bacterial ferredoxin reductase, whereas the Fpr protein may be a subclass I bacterial ferredoxin. It was very interesting to examine the evolutionary acquisition of these two different types of ferredoxin reductases in the *P. putida* genome, as most other bacteria only appear to have one ferredoxin reductase [5].

Purification and Diaphorase Activity Assay of FprB

The purified FprB migrated as a single band with an apparent molecular mass of ~29 kDa, as estimated by SDS-PAGE (Fig. 2A), which agreed well with the calculated value (28,595 Da). The molecular mass of the native FprB was estimated to be about 35 kDa based on size exclusion chromatography (Fig. 2B). It has already been shown that a number of Fpr proteins have a monomeric structure under native conditions, although there are some exceptions [28], and the present data also indicated that the purified native FprB existed as a monomeric protein. The FprB

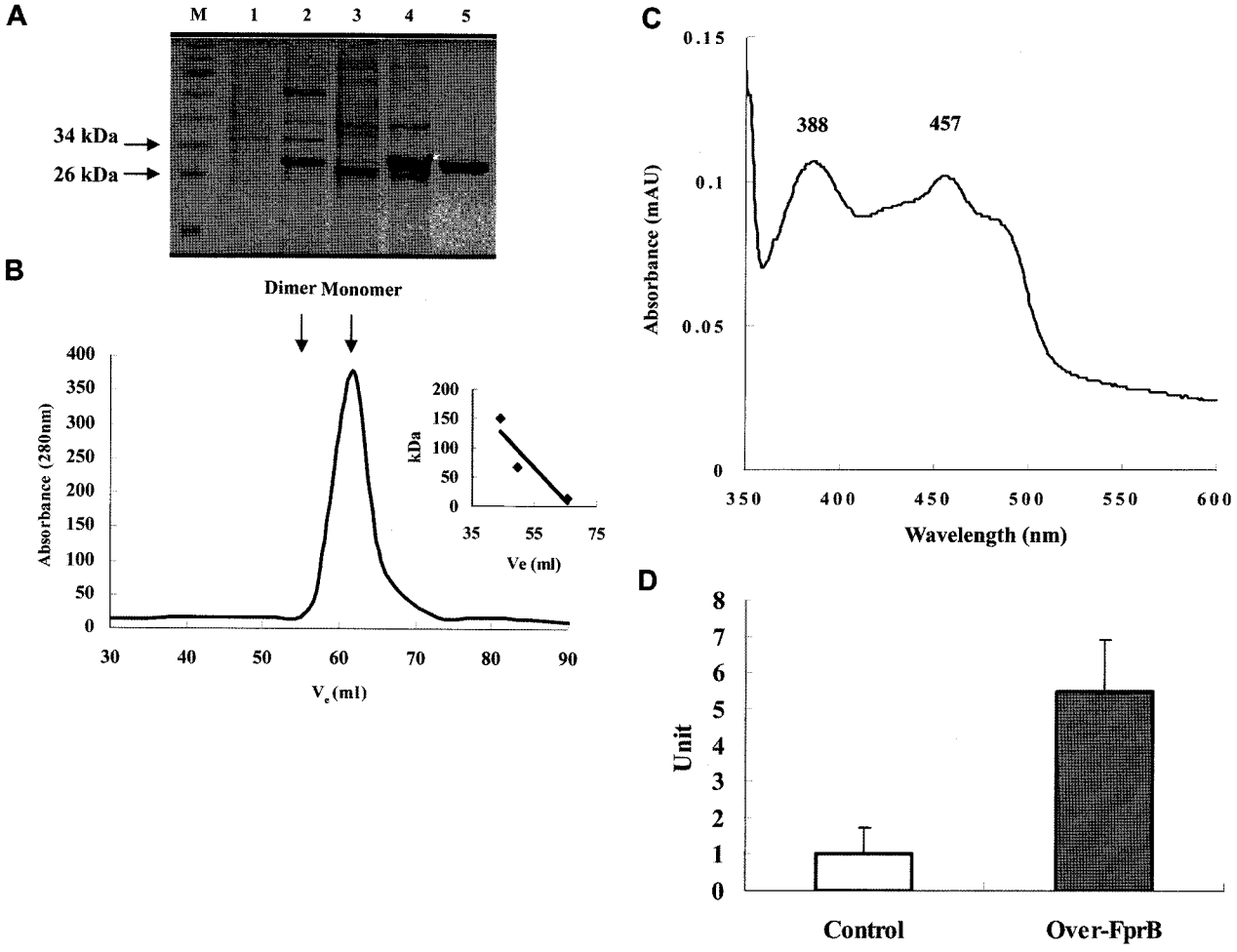

Fig. 2. A. Purification of recombinant FprB, as analyzed by SDS-PAGE. Lane M, Molecular marker (values are indicated in kDa); lane 1, IPTG untreated; lane 2, crude extract; lane 3, elution product using DEAE anion-exchange column; lane 4, elution product using Sephacryl gel-filtration column; lane 5, concentrate of elution product using ultrafiltration (Amicon, YM-10). **B.** Size exclusion chromatography of purified FprB. The inner square indicates the size exclusion chromatography standard based on alcohol dehydrogenase, bovine serum albumin, and lysozyme. **C.** Spectral analysis using anion-exchange-column-purified FprB. The mixture contained 50 mM Tris/Cl (pH 8.0) and 10% (v/v) glycerol. **D.** Diaphorase activity assay using wild-type cells (control, white bar) and FprB-overexpression strain (Over-FprB, grey bar). The diaphorase activity unit is defined as ΔOD_{600}/min/ng protein.

size was very similar to that of the purified Fpr (~30 kDa) from *Rhodobacter capsulatus* [2] and purified *E. coli* Fpr (~29 kDa) [22], yet much smaller than those of *Chlorobium tepidum* (42 kDa), *Bacillus subtilis* (40 kDa), and *Mycobacterium tuberculosis* (50 kDa) [28]. It is already known that flavoproteins, which include an FAD cofactor, have bands centered at 360–390 nm and 440–470 nm within their absorption spectrum, depending on the protein environment [9]. The purified FprB also exhibited the same pattern as a flavoprotein (Fig. 2C) with two absorption maxima at ~388 nm and ~457 nm (Fig. 2C). Fpr is also known to have diaphorase activity, which drives electron transfer from NADPH to a wide variety of artificial electron acceptors [9]. Thus, a diaphorase activity assay using the soluble fractions of the cell lysate was performed to demonstrate the function of FprB, where DPIP and NADPH were used as the artificial electron acceptor and donor, respectively. A quantitative comparison of the diaphorase activities, measured using the wild-type and FprB-overexpressed cells, is shown in Fig. 2D. The DPIP-reducing ability of the FprB-overexpressed cells was five-fold greater than that of the wild-type cells (Fig. 2D). Thus, when taken together, FprB was annotated as a ferredoxin-$NADP^+$ reductase.

Expression Analysis of *fprB* Under Various Conditions

The promoter activity of the *fpr* gene is much higher during exponential growth than during stationary growth [21, 26]. However, in this study, a Northern blot analysis indicated that the *fprB* promoter activity was only slightly induced during exponential growth (Fig. 3A). In contrast to the expression profile of the *fpr* gene, there was no change in the level of *fprB* expression with various concentrations of oxidative stress agents, such as paraquat, menadione, hydrogen peroxide, and *t*-butyl hydroperoxide (*t*-BOOH) (data not shown). Interestingly, a higher level of *fprB* expression was only observed under osmotic stress conditions (Fig. 3B). As bacterial growth is severely inhibited during continuous growth in an LB medium containing high NaCl [6], *P. putida* KT2440 was exposed to osmotic shock for either 5 or 10 min to examine the osmotic effects on *fprB* expression. After the *P. putida* cells had been grown overnight in NaCl-free LB media, the cultures were diluted 100-fold in 10 ml of a fresh NaCl-free LB medium, and then grown to an OD_{600} of around 0.2. Thereafter, the cells were divided into five tubes containing LB media with various concentrations of NaCl. The final concentrations of NaCl in the LB were 0, 0.51, and 0.85 M, respectively. A Northern blot analysis was conducted after collecting the total RNA from the cells, and an increase in *fprB* expression was found in both the 0.51 and 0.85 M NaCl LB media (Fig. 3B).

However, a further analysis of the promoter region of *fprB* is required, as the reason for the existence of

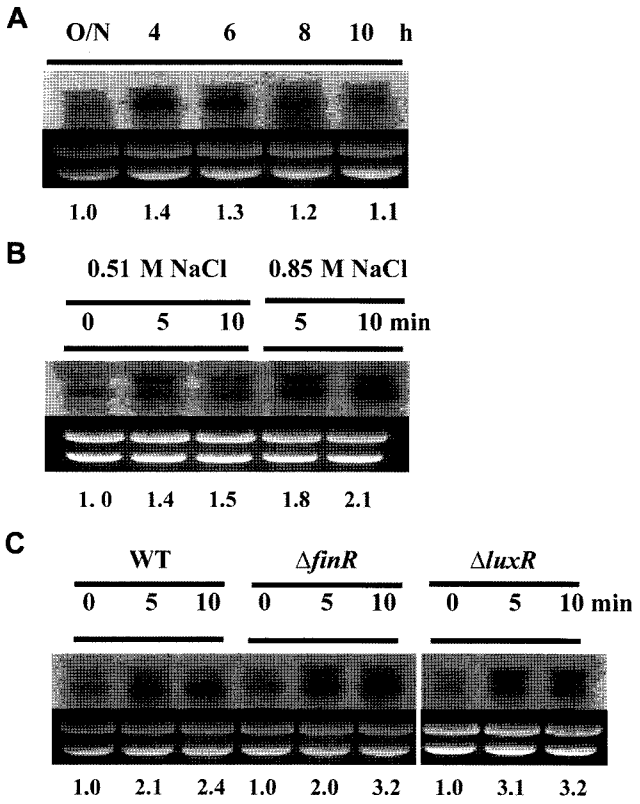

Fig. 3. Northern blot analysis of the *fprB* gene under various conditions.

A. Growth phase-dependent expression of *fprB*; O/N, overnight culture (16 h); incubation time (min) is shown in each panel. **B**. Induction of *fprB* gene by osmotic stress. **C**. Induction of *fprB* is independent of FinR and LuxR. The ethidium bromide (EtBr) stained gel prior to blotting demonstrated consistent loading in all lanes. The intensity ratio, shown below EtBr, indicates the fold difference relative to the control, as established by a densitometric analysis (Kodak 1D ver.3.6.1)

two bands in the Northern blot analysis was unclear. *P. putida* KT2440-P_{fprB}-lacZ and *P. putida* KT2440 (pRK415-P_{fprB}) were used to monitor the expression of the *fprB* gene. Measurements of the β-galactosidase activity and GFP fluorescence were conducted to confirm the expression of the *fprB* promoter in the presence of high concentrations of NaCl. Consistent with the Northern blot data, the level of *fprB-lacZ* expression was about 3.78-fold higher [Miller unit: 0 M NaCl (16.81±0.02), 0.85 M NaCl (64.53±1.47)] at high NaCl concentrations than under NaCl-free LB conditions (Miller unit). The amount of GFP expressed increased in the presence of a high concentration of NaCl (0.85 M), and was 1.32-fold higher than without NaCl [fluorescence intensity: 0 M NaCl (726.91±1.64), 0.85 M NaCl (960.63±19.41)]. Therefore, the collective data only indicated a slight increase in *fprB* expression, yet significant increase under osmotic stress conditions. FinR, a transcriptional activator of *fpr* and LuxR-type transcriptional factor near the *fprB* region, seemed unlikely to be involved in the induction of *fprB* under osmotic

conditions, as the deletion of either *finR* or *luxR* did not affect the expression pattern of *fprB* (Fig. 3C). Thus, an unknown regulator for the control of *fprB* in the presence of high osmotic stress may exist, meaning further molecular characterization of *fprB* expression is essential to understand its regulation.

Growth Defect of *fprB* Mutant Under Osmotic Stress Conditions

The aerobic growth rates of both the wild type (1.91±0.07 h^{-1}) and *fprB* mutant (1.71±0.21 h^{-1}) were very similar in LB liquid media. However, comparing their growth rates under osmotic stress conditions revealed that the *fprB* mutant had a growth defect in an LB liquid medium (Fig. 4A). After the wild-type and mutant cells were grown overnight in NaCl-free LB media, ~10^7 cells were inoculated into 50 ml of fresh LB media with either NaCl (0.85 M), KCl (0.85 M), or sucrose (1.0 M). After inoculation, the growth was observed by measuring the optical density at 600 nm with a spectrophotometer. The specific growth rates of the wild-type and mutant cells were 0.85±0.12 and 0.67±0.18 h^{-1}, respectively, in the LB media with NaCl (0.85 M), whereas in the presence of KCl (0.85 M), the specific growth rates were 0.67±0.11 and 0.45±0.01 h^{-1}, respectively. A high concentration of sucrose had no affect on the growth rate of either cell type, although the *fprB* mutant exhibited a longer lag phase than the wild-type cells (data not shown). Consistent with the expression of *fprB* being unaffected by the presence of oxidative stress agents, there was no difference in the aerobic growth rates between the wild and *fprB* mutant types in the presence or absence of various concentrations of paraquat (data not shown). To test their plate growth, a culture grown overnight in an NaCl-free LB medium was diluted 100-fold in 5 ml of a fresh NaCl-free LB medium, and then grown to an OD_{600} of approximately 0.4. The exponentially grown (~10^8 cells) cells of each strain were then serially diluted and spotted onto LB agar plates in the presence and absence of NaCl, KCl, and sucrose. The *fprB* mutant cells exhibited a growth defect in the presence of high salts, as shown in Fig. 4B. Thus, when taken together with the involvement of the *fpr* gene against osmotic stress, this result strongly suggests that ferredoxin-$NADP^+$ reductases play an important role in protecting cells under high osmotic conditions [21]. Although the serial dilution did not produce any obvious growth defect for the mutant cells in the presence of high sucrose, the colony sizes in each spot were smaller than those of the wild-type cells (data not shown).

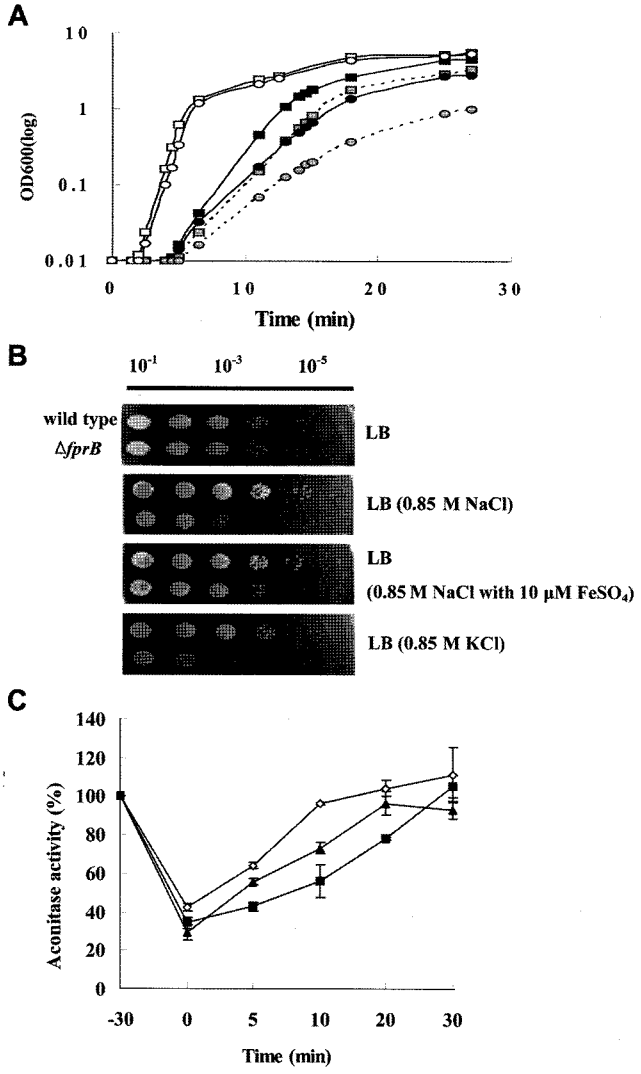

Fig. 4. **A.** Growth curves for wild-type (square) and *fprB* mutant (circle) in LB media with osmotic stress agents: open square circle (LB medium), black (LB medium with 0.85 M NaCl), and dotted line with grey color (LB medium with 0.85 M KCl). **B.** Phenotypic assays of wild-type and mutant strains of *P. putida* KT2440. **C.** Aconitase activities in *P. putida* cells [the wild-type (◇), *fpr* (■), or *fprB* (▲)]. The bars represent the means and standard deviations of three determinations.

Soil bacteria often experience fluctuations in the osmolality of their habitat owing to drying and flooding of the upper layers of the soil [3]. A rise in the external salinity and osmolality triggers an outflow of water from the cells, resulting in reduced turgidity and dehydration of the cytoplasm. When bacterial cells are continuously growing under high saline conditions, iron limitation occurs inside the cells, triggering the derepression of a variety of iron-controlled genes [13]. It has been assumed that high-salinity-stressed bacterial cells experience iron deficiency, suggesting that the growth retardation exhibited by these cultures should at least be partially compensated for by a substantial increase in the iron concentration of the growth medium [13]. Thus, to test this hypothesis, the growth of the *fprB* mutant and wild-type cells of *P. putida* KT2440 was monitored under high salinity (0.85 M NaCl) in the presence of 10 μM $FeSO_4$ (Fig. 4B). Iron supplementation on an LB plate containing NaCl (0.85 M) resulted in substantially better

cell growth of both the wild-type and the *fprB* mutant compared with cultures in the absence of iron (Fig. 4B).

Recovery of Aconitase Activities

It has already been demonstrated that the catalytic iron-sulfur clusters in the hydrolyase of *E. coli* are inactivated when the cells are exposed to excessive superoxide [1], yet Fpr can repair oxidatively damaged proteins [10]. Thus, to investigate whether Fpr is involved in the recovery of oxidatively damaged aconitase, an iron-sulfur cluster containing hydrolyase and the wild or *fpr* mutant types was treated with paraquat for 30 min, and then transferred to paraquat-free LB media to measure the aconitase activity over time. After oxidative stress, the aconitase activity of the wild type was quickly regenerated to 100% within 10 min. However, the recovery of the aconitase activities of the *fpr* and *fprB* mutants was much slower, with complete regeneration taking 20 min or more (Fig. 4C), confirming that Fpr and FprB were both engaged in the recovery of the oxidatively damaged aconitase. These results also indicated that there may be kinetic differences between the Fpr and FprB proteins, as expected from the amino acid sequence analyses (Fig. 1B). The subclass I bacterial ferredoxin reductase, Fpr, worked more effectively on the repair process when compared with the subclass II FprB. Thus, when taken together, the above data showed that the *fprB* gene encoded a functional FprB protein and was required for cell recovery under oxidative stress conditions, although its expression was not induced under oxidative stress conditions. Furthermore, this study, along with previous observations [21], showed that *fpr* and *fprB* are both highly inducible under high osmotic conditions and play an important role in protecting cells from osmotic stress. The catalytic function of FprB may have evolved to augment the function of Fpr in *P. putida* KT2440, especially under osmotic stress.

It is speculated that more reactive oxygen species are generated during metabolism under high osmotic conditions, which is supported by the fact that many proteomics studies under osmotic conditions have detected high levels of oxidative-stress-defense gene expression [14, 25], plus the expressions of the antioxidant genes *soxS* and *katE* are significantly induced by an increase in osmolarity [29]. Interestingly, strains of *P. aeruginosa* and *Streptomyces coelicolor* that lack functional catalases have been reported to be more sensitive to osmotic stress than the wild-type strains [7], suggesting cross-talk between oxidative and osmotic stress response circuits. However, the molecular basis for the regulatory link between these stresses remains to be elucidated.

Acknowledgments

This work was supported by an NCRC (National Core Research Center) grant (R15-2003-012-02002-0) and a grant (R0503442) from the BioGreen21 Program, Republic of Korea to WP. Yunho Lee and Jinki Yeom contributed equally to this work.

References

1. Abranches, J., J. A. Lemos, and B. A. Burne. 2006. Osmotic stress responses of *Streptococcus mutas* UA159. *FEMS Microbiol. Lett.* **255:** 240–246.
2. Bittel, C., L. C. Tabares, M. Armesto, N. Carrillo, and N. Cortez. 2003. The oxidant-responsive diaphorease of *Rhodobacter capsulatus* in a ferredoxin (flavodoxin)-NADP(H) reductase. *FEBS Lett.* **553:** 408–412.
3. Bremer, E. and R. Krämer. 2000. Coping with osmotic challenges: Osmoregulation through accumulation and release of compatible solutes in bacteria, pp. 79–97. *In* G. Storz and R. Hengge-Aronis (eds.), *Bacterial Stress Responses*. ASM Press, Washington DC.
4. Carrillo, N. and E. A. Ceccarelli. 2003. Open questions in ferredoxin-NADP$^+$ reductase catalytic mechanism. *Eur. J. Biochem.* **270:** 1900–1915.
5. Ceccarelli, E. A., A. K. Arakaki, N. Cortez, and N. Carrillo. 2004. Functional plasticity and catalytic efficiency in plant and bacterial ferredoxin-NADP(H) reductase. *Biochim. Biophys. Acta* **1698:** 155–165.
6. Cheung, K. J., V. Badarinarayana, D. W. Selinger, D. Janes, and G. A. Church. 2003. A microarray-based antibiotic screen identifies a regulatory role for supercoiling in the osmotic stress response of *Escherichia coli*. *Genome Res.* **13:** 206–215.
7. Cho, Y. H., E. J. Lee, and J. H. Roe. 2000. A developmentally regulated catalase required for proper differentiation and osmoprotection of *Streptomyces coelicolor*. *Mol. Microbiol.* **35:** 150–160.
8. Djaman, O., F. W. Outten, and J. A. Imlay. 2004. Repair of oxidized iron-sulfur cluster in *Escherichia coli*. *J. Biol. Chem.* **279:** 44590–44599.
9. Fischer, F., D. Raimondi, A. Aliverti, and G. Zanetti. 2002. *Mycobacterium tuberculosis* FprA, a novel bacterial NADPH-ferredoxin reductase. *Eur. J. Biochem.* **269:** 3005–3013.
10. Giro, M., N. Carrillo, and A. R. Krapp. 2006. Glucose-6-phosphate dehydrogenase and ferredoxin-NADP(H) reductase contribute to damage repair during the *soxRS* response of *Escherichia coli*. *Microbiology* **152:** 1119–1128.
11. Greenberg, J., P. Monach, J. Chou, D. Josepphy, and B. Demple. 1990. Positive control of a global antioxidant defense regulon activated by superoxide-generating agents in *Escherichia coli*. *Proc. Natl. Acad. Sci. USA* **87:** 6181–6185.
12. Griffith, K. L. and R. E. Wolf. 2001. Systematic mutagenesis of the DNA binding sites for SoxS in the *Escherichia coli zwf* and *fpr* promoters: Identifying nucleotides required for DNA binding and transcription activation. *Mol. Microbiol.* **40:** 1141–1154.
13. Hoffmann, T., A. Schutz, M. Brosius, A. Volker, U. Volker, and E. Bremer. 2002. High-salinity-induced iron limitation in *Bacillus subtilis*. *J. Bacteriol.* **184:** 718–727.

14. Höpper, D., J. Bernhardt, and M. Hecker. 2006. Salt stress adaptation of *Bacillus subtilis*: A physiological proteomics approach. *Proteomics* **6:** 1550–1562.
15. Imlay, J. A. 2003. Pathways of oxidative damage. *Annu. Rev. Microbiol.* **57:** 395–418.
16. Jeong, E., K. Park, S. Y. Yi, H. Kang, S. J. Chung, C. Lee, J. W. Chung, D. Seol, B. H. Chung, and M. Kim. 2007. Stress-governed expression and purification of human type II hexokinase in *Escherichia coli*. *J. Microbiol. Biotechnol.* **17:** 638–643.
17. Kalogeraki, V. S. and S. C. Winans. 1997. Suicide plasmids containing promoterless reporter genes can simultaneously disrupt and create fusions to target genes of diverse bacteria. *Gene* **188:** 69–75.
18. Kang, Y.-S., Y. J. Kim, C. O. Jeon, and W. Park. 2006. Characterization of naphthalene-degrading *Pseudomonas* species isolated from pollutant-contaminated sites: Oxidative stress during their growth on naphthalene. *J. Microbiol. Biotechnol.* **16:** 1819–1825
19. Krapp, A. R., T. B. Tognetti, N. Carrillo, and A. Acevedo. 1997. The role of ferredoxin-NADP+ reductase in the concerted cell defense against oxidative damage - studies using *Escherichia coli* mutants and cloned plant genes. *Eur. J. Biochem.* **249:** 556–563.
20. Lee, Y., E. Ahn, S. Park, E. L. Madsen, C. O. Jeon, and W. Park. 2006. Construction of a reporter strain *Pseudomonas putida* for the detection of oxidative stress caused by environmental pollutants. *J. Microbiol. Biotechnol.* **16:** 386–390.
21. Lee, Y., S. Pena-Llopis, Y. S. Kang, H. D. Shin, B. Demple, E. L. Madsen, C. O. Jeon, and W. Park. 2006. Expression analysis of the *fpr* (ferredoxin-NADP$^+$ reductase) gene in *Pseudomonas putida* KT2440. *Biochem. Biophys. Res. Commun.* **339:** 1246–1254.
22. Li, Z. and B. Demple. 1996. Sequence specificity for DNA binding by *Escherichia coli* SoxS and Rob proteins. *Mol. Microbiol.* **20:** 937–945.
23. Miller, J. H. 1972. *Experiments in Molecular Genetics*. Cold Spring Harbor Laboratory Press, Cold Spring Harbor, NY.
24. Oka, A., H. Sugisaki, and M. Takanami. 1981. Nucleotide sequence of the kanamycin resistance transposon Tn903. *J. Mol. Biol.* **147:** 217–226.
25. Pané-Farré, J., B. Jonas, K. Förstner, S. Engelmann, and M. Hecker. 2006. The σ^B regulon in *Staphylococcus aureus* and its regulation. *Int. J. Med. Microbiol.* **296:** 237–258.
26. Park, W., S. Pena-Llopis, Y. Lee, and B. Demple. 2006. Regulation of superoxide stress in *Pseudomonas putida* KT2440 is different from the SoxR paradigm in *Escherichia coli*. *Biochem. Biophys. Res. Commun.* **341:** 51–56.
27. Philippe, N., J. P. Alcaraz, E. Coursange, J. Geiselmann, and D. Schneider. 2004. Improvement of pCVD442, a suicide plasmid for gene allele exchange in bacteria. *Plasmid* **51:** 246–255.
28. Seo, D. and H. Sakurai. 2002. Purification and characterization of ferredoxin-NAD(P)+ reductase from the green sulfur bacterium *Chlorobium tepidum*. *Biochim. Biophys. Acta* **1597:** 123–132.
29. Smirnova, G. V., N. G. Muzyka, and O. N. Oktyabrsky. 2000. The role of antioxidant enzymes in response of *Escherichia coli* to osmotic upshift. *FEMS Microbiol. Lett.* **186:** 209–213.
30. Wackett, L. P. 2003. *Pseudomonas putida* -- a versatile biocatalyst. *Nature Biotechnol.* **21:** 136–138.
31. Yin, S., M. Fuangthong, W. P. Laratta, and J. P. Shapleigh. 2003. Use of a green fluorescent protein-based reporter fusion for detection of nitric oxide produced by denitrifiers. *Appl. Environ. Microbiol.* **69:** 3938–3944.
32. Yu, T. S. 2005. Purification and characterization of pyrimidine nucleotide N-ribosidase from *Pseudomonas oleovorans*. *J. Microbiol. Biotechnol.* **15:** 573–578.